EUROPEAN ORGANIZATION FOR NUCLEAR RESEARCH

CERN-EP/2001-021
February 28, 2001

# A Combination of Preliminary Electroweak Measurements and Constraints on the Standard Model

**The LEP Collaborations* ALEPH, DELPHI, L3, OPAL, the LEP Electroweak Working Group† and the SLD Heavy Flavour and Electroweak Groups‡**

**Prepared from Contributions of the LEP and SLD experiments to the 2000 Summer conferences.**

**Abstract**

This note presents a combination of published and preliminary electroweak results from the four LEP collaborations and the SLD collaboration which were prepared for the 2000 summer conferences. Averages from Z resonance results are derived for hadronic and leptonic cross sections, the leptonic forward-backward asymmetries, the $\tau$ polarisation asymmetries, the $b\overline{b}$ and $c\overline{c}$ partial widths and forward-backward asymmetries and the $q\overline{q}$ charge asymmetry. Above the Z resonance, averages are derived for di–fermion cross sections and asymmetries, W–pair, Z–pair and single–W production cross section, electroweak gauge boson couplings and W mass and decay branching ratios. The major changes with respect to results presented in summer 1999 are final Z lineshape results from LEP, updates to the W mass and gauge-boson couplings from LEP, and $A_{\rm LR}$ from SLD. The results are compared with precise electroweak measurements from other experiments. The parameters of the Standard Model are evaluated, first using the combined LEP electroweak measurements, and then using the full set of electroweak results.

*The LEP Collaborations each take responsibility for the preliminary results of their own.

†The members of the LEP Electroweak Working Group who contributed significantly to this note are : D. Abbaneo, J. Alcaraz, P. Antilogus, S. Arcelli, P. Bambade, E. Barberio, G. Bella, A. Blondel, S. Blyth, D. Bourilkov, R. Chierici, R. Clare, P. de Jong, G. Duckeck, A. Ealet, M. Elsing, F. Fiedler, P. Garcia-Abia, A. Gurtu, M.W. Grünewald, J.B. Hansen, R. Hawkings, J. Holt, S. Jezequel, R.W.L. Jones, N. Kjaer, M. Kobel, E. Lançon, W. Lohmann, C. Mariotti, M. Martinez, F. Matorras, C. Matteuzzi, S. Mele, E. Migliore, M.N. Minard, K. Mönig, A. Olshevski, C. Parkes, U. Parzefall, Ch. Paus, M. Pepe-Altarelli, B. Pietrzyk, G. Quast, P. Renton, H. Rick, S. Riemann, J.M. Roney, K. Sachs, C. Sbarra, A. Schmidt-Kaerst, S. Spagnolo, A. Straessner, R. Ströhmer D. Strom, R. Tenchini, F. Terranova, F. Teubert, M.A. Thomson, E. Tournefier, M. Verzocchi, H. Voss, C.P. Ward, St. Wynhoff.

‡T. Abe, N. de Groot, M. Iwasaki, P.C. Rowson, D. Su, M. Swartz.

# 1 Introduction

The four LEP experiments and SLD have previously presented [1] parameters derived from the Z resonance using published and preliminary results based on data recorded until the end of 1995 for the LEP experiments and 1998 for SLD. Since 1996 LEP has run at energies above the W-pair production threshold. In 1999 the delivered luminosity was significantly higher than in previous years, and thus the knowledge of the properties of the W boson has been significantly improved. To allow a quick assessment, a box highlighting the updates is given at the beginning of each section.

LEP-I (1990-1995) Z-pole measurements are the hadronic and leptonic cross sections, the leptonic forward-backward asymmetries, the $\tau$ polarisation asymmetries, the $\mathrm{b\overline{b}}$ and $\mathrm{c\overline{c}}$ partial widths and forward-backward asymmetries and the $\mathrm{q\overline{q}}$ charge asymmetry. The measurements of the left-right cross section asymmetry, the $\mathrm{b\overline{b}}$ and $\mathrm{c\overline{c}}$ partial widths and left-right-forward-backward asymmetries for b and c quarks from SLD are treated consistently with the LEP data. Many technical aspects of their combination are described in References 2, 3 and references therein.

The LEP-II (1996-2000) measurements are di–fermion cross sections and asymmetries; W–pair, Z–pair and single–W production cross sections, electroweak gauge boson couplings. W boson properties, like mass, width and decay branching ratios are also measured.

Several measurements included in the combinations are still preliminary.

This note is organised as follows:

**Section 2** Z Line Shape and Leptonic Forward-Backward Asymmetries;

**Section 3** $\tau$ Polarisation;

**Section 4** $A_{\mathrm{LR}}$ Measurement at SLD;

**Section 5** Heavy Flavour Analyses;

**Section 6** Inclusive Hadronic Charge Asymmetry;

**Section 7** $\mathrm{f\overline{f}}$ Production at Energies above the Z;

**Section 8** W Boson Properties, including $m_{\mathrm{W}}$, Branching Ratios, W–pair Production Cross Section;

**Section 9** Single–W Production Cross Section;

**Section 10** ZZ Production Cross Section;

**Section 11** Electroweak Gauge Boson Couplings;

**Section 12** Interpretation of the Results, Including the Combination of Results from LEP, SLD, Neutrino Interaction Experiments and from CDF and DØ;

**Section 13** Prospects for the Future.

## 2 Results from the Z Peak Data

**Updates with respect to last summer:**
All experiments have updated their results, and all are now final. Recent theoretical developments have been included in the results and fits.

### 2.1 Z Lineshape and Lepton Forward-Backward Asymmetries

The results presented here are based on the full LEP-I data set. This includes the data taken during the energy scans in 1990 and 1991 in the range[1] $|\sqrt{s} - m_{\mathrm{Z}}| < 3$ GeV, the data collected at the Z peak in 1992 and 1994 and the precise energy scans in 1993 and 1995 ($|\sqrt{s} - m_{\mathrm{Z}}| < 1.8$ GeV). The total event statistics are given in Table 1. Details of the individual analyses can be found in References 4–7.

| $\mathrm{q\overline{q}}$ | | | | | |
|---|---|---|---|---|---|
| year | A | D | L | O | all |
| '90/91 | 433 | 357 | 416 | 454 | 1660 |
| '92 | 633 | 697 | 678 | 733 | 2741 |
| '93 | 630 | 682 | 646 | 649 | 2607 |
| '94 | 1640 | 1310 | 1359 | 1601 | 5910 |
| '95 | 735 | 659 | 526 | 659 | 2579 |
| total | 4071 | 3705 | 3625 | 4096 | 15497 |

| $\ell^+\ell^-$ | | | | | |
|---|---|---|---|---|---|
| year | A | D | L | O | all |
| '90/91 | 53 | 36 | 39 | 58 | 186 |
| '92 | 77 | 70 | 59 | 88 | 294 |
| '93 | 78 | 75 | 64 | 79 | 296 |
| '94 | 202 | 137 | 127 | 191 | 657 |
| '95 | 90 | 66 | 54 | 81 | 291 |
| total | 500 | 384 | 343 | 497 | 1724 |

Table 1: The $\mathrm{q\overline{q}}$ and $\ell^+\ell^-$ event statistics, in units of $10^3$, used for the analysis of the Z line shape and lepton forward-backward asymmetries by the experiments ALEPH (A), DELPHI (D), L3 (L) and OPAL (O).

For the averaging of results the LEP experiments provide a standard set of 9 parameters describing the information contained in hadronic and leptonic cross sections and leptonic forward-backward asymmetries. These parameters are convenient for fitting and averaging since they have small correlations. They are:

- The mass and total width of the Z boson, where the definition is based on the Breit-Wigner denominator $(s - m_{\mathrm{Z}}^2 + is\Gamma_{\mathrm{Z}}/m_{\mathrm{Z}})$ with $s$-dependent width [8].
- The hadronic pole cross section of Z exchange:

$$\sigma_{\mathrm{h}}^0 \equiv \frac{12\pi}{m_{\mathrm{Z}}^2}\frac{\Gamma_{\mathrm{ee}}\Gamma_{\mathrm{had}}}{\Gamma_{\mathrm{Z}}^2}\,. \tag{1}$$

  Here $\Gamma_{\mathrm{ee}}$ and $\Gamma_{\mathrm{had}}$ are the partial widths of the Z for decays into electrons and hadrons.

- The ratios:

$$R_{\mathrm{e}} \equiv \Gamma_{\mathrm{had}}/\Gamma_{\mathrm{ee}}, \quad R_\mu \equiv \Gamma_{\mathrm{had}}/\Gamma_{\mu\mu} \text{ and } R_\tau \equiv \Gamma_{\mathrm{had}}/\Gamma_{\tau\tau}. \tag{2}$$

  Here $\Gamma_{\mu\mu}$ and $\Gamma_{\tau\tau}$ are the partial widths of the Z for the decays $\mathrm{Z} \to \mu^+\mu^-$ and $\mathrm{Z} \to \tau^+\tau^-$. Due to the mass of the $\tau$ lepton, a difference of 0.2% is expected between the values for $R_{\mathrm{e}}$ and $R_\mu$, and the value for $R_\tau$, even under the assumption of lepton universality [9].

[1] In this note $\hbar = c = 1$.

- The pole asymmetries, $A_{\rm FB}^{0,\,\rm e}$, $A_{\rm FB}^{0,\,\mu}$ and $A_{\rm FB}^{0,\,\tau}$, for the processes $\rm e^+e^- \to e^+e^-$, $\rm e^+e^- \to \mu^+\mu^-$ and $\rm e^+e^- \to \tau^+\tau^-$. In terms of the real parts of the effective vector and axial-vector neutral current couplings of fermions, $g_{V\rm f}$ and $g_{A\rm f}$, the pole asymmetries are expressed as

$$A_{\rm FB}^{0,\,\rm f} \equiv \frac{3}{4}\mathcal{A}_{\rm e}\mathcal{A}_{\rm f} \tag{3}$$

with

$$\mathcal{A}_{\rm f} \equiv \frac{2g_{V\rm f}g_{A\rm f}}{g_{V\rm f}^2+g_{A\rm f}^2} = 2\frac{g_{V\rm f}/g_{A\rm f}}{1+(g_{V\rm f}/g_{A\rm f})^2}\,. \tag{4}$$

The imaginary parts of the vector and axial-vector coupling constants as well as real and imaginary parts of the photon vacuum polarisation are taken into account explicitly in the fitting formulae and are fixed to their Standard Model values. The fitting procedure takes into account the effects of initial-state radiation [8] to $\mathcal{O}(\alpha^3)$ [10–12], as well as the $t$-channel and the $s$-$t$ interference contributions in the case of $\rm e^+e^-$ final states.

The set of 9 parameters does not describe hadron and lepton-pair production completely, because it does not include the interference of the $s$-channel Z exchange with the $s$-channel $\gamma$ exchange. For the results presented in this section and used in the rest of the note, the $\gamma$-exchange contributions and the hadronic $\gamma$Z interference terms are fixed to their Standard Model values. The leptonic $\gamma$Z interference terms are expressed in terms of the effective couplings.

The four sets of 9 parameters provided by the LEP experiments are presented in Table 2. For performing the average over these four sets of nine parameters, the overall covariance matrix is constructed from the covariance matrices of the individual LEP experiments and common systematic errors [2]. The common systematic errors include theoretical errors as well as errors arising from the uncertainty in the LEP beam energy. The beam energy uncertainty contributes an uncertainty of $\pm1.7$ MeV to $m_{\rm Z}$ and $\pm1.2$ MeV to $\Gamma_{\rm Z}$. In addition, the uncertainty in the centre-of-mass energy spread of about $\pm1$ MeV contributes $\pm0.2$ MeV to $\Gamma_{\rm Z}$. The theoretical error on calculations of the small-angle Bhabha cross section is $\pm0.054\,\%$ [13] for OPAL and $\pm0.061\,\%$ [14] for all other experiments, and results in the largest common systematic uncertainty on $\sigma_{\rm h}^0$. QED radiation, dominated by photon radiation from the initial state electrons, contributes a common uncertainty of $\pm0.02\,\%$ on $\sigma_{\rm h}^0$, of $\pm0.3$ MeV on $m_{\rm Z}$ and of $\pm0.2$ MeV on $\Gamma_{\rm Z}$. The contribution of $t$-channel diagrams and the $s$-$t$ interference in $\rm Z \to e^+e^-$ leads to an additional theoretical uncertainty estimated to be $\pm0.24$ on $R_{\rm e}$ and $\pm0.0014$ on $A_{\rm FB}^{0,\,\rm e}$, which are fully anti–correlated. Uncertainties from the model-independent parameterisation of the energy dependence of the cross section are almost negligible, if the definitions of Reference [15] are applied. Through unavoidable Standard Model remnants, dominated by the need to fix the $\gamma$-Z interference contribution in the $\rm q\overline{q}$ channel, there is some small dependence of $\pm0.2$ MeV of $m_{\rm Z}$ on the Higgs mass, $m_{\rm H}$ (in the range 100 GeV to 1000 GeV) and the value of the electromagnetic coupling constant. Such "parametric" errors are negligible for the other pseudo-observables. The combined parameter set and its correlation matrix are given in Table 3.

If lepton universality is assumed, the set of 9 parameters is reduced to a set of 5 parameters. $R_\ell$ is defined as $R_\ell \equiv \Gamma_{\rm had}/\Gamma_{\ell\ell}$, where $\Gamma_{\ell\ell}$ refers to the partial Z width for the decay into a pair of massless charged leptons. The data of each of the four LEP experiments are consistent with lepton universality (the difference in $\chi^2$ over the difference in d.o.f. with and without the assumption of lepton universality is 3/4, 6/4, 5/4 and 3/4 for ALEPH, DELPHI, L3 and OPAL, respectively). The lower part of Table 3 gives the combined result and the corresponding correlation matrix. Figure 1 shows, for each lepton species and for the combination assuming lepton universality, the resulting 68% probability contours in the $R_\ell$-$A_{\rm FB}^{0,\,\ell}$ plane. Good agreement is observed.

| | | correlations | | | | | | | | |
|---|---|---|---|---|---|---|---|---|---|---|
| | | $m_{\rm Z}$ | $\Gamma_{\rm Z}$ | $\sigma^0_{\rm h}$ | $R_{\rm e}$ | $R_\mu$ | $R_\tau$ | $A^{0,{\rm e}}_{\rm FB}$ | $A^{0,\mu}_{\rm FB}$ | $A^{0,\tau}_{\rm FB}$ |
| $\chi^2/N_{{\rm d}f}$ = 169/176 | | | | | ALEPH | | | | | |
| $m_{\rm Z}$ [GeV] | 91.1891 ± 0.0031 | 1.00 | | | | | | | | |
| $\Gamma_{\rm Z}$ [GeV] | 2.4959 ± 0.0043 | .038 | 1.00 | | | | | | | |
| $\sigma^0_{\rm h}$ [nb] | 41.558 ± 0.057 | −.091 | −.383 | 1.00 | | | | | | |
| $R_{\rm e}$ | 20.690 ± 0.075 | .102 | .004 | .134 | 1.00 | | | | | |
| $R_\mu$ | 20.801 ± 0.056 | −.003 | .012 | .167 | .083 | 1.00 | | | | |
| $R_\tau$ | 20.708 ± 0.062 | −.003 | .004 | .152 | .067 | .093 | 1.00 | | | |
| $A^{0,{\rm e}}_{\rm FB}$ | 0.0184 ± 0.0034 | −.047 | .000 | −.003 | −.388 | .000 | .000 | 1.00 | | |
| $A^{0,\mu}_{\rm FB}$ | 0.0172 ± 0.0024 | .072 | .002 | .002 | .019 | .013 | .000 | −.008 | 1.00 | |
| $A^{0,\tau}_{\rm FB}$ | 0.0170 ± 0.0028 | .061 | .002 | .002 | .017 | .000 | .011 | −.007 | .016 | 1.00 |
| $\chi^2/N_{{\rm d}f}$ = 177/168 | | | | | DELPHI | | | | | |
| $m_{\rm Z}$ [GeV] | 91.1864 ± 0.0028 | 1.00 | | | | | | | | |
| $\Gamma_{\rm Z}$ [GeV] | 2.4876 ± 0.0041 | .047 | 1.00 | | | | | | | |
| $\sigma^0_{\rm h}$ [nb] | 41.578 ± 0.069 | −.070 | −.270 | 1.00 | | | | | | |
| $R_{\rm e}$ | 20.88 ± 0.12 | .063 | .000 | .120 | 1.00 | | | | | |
| $R_\mu$ | 20.650 ± 0.076 | −.003 | −.007 | .191 | .054 | 1.00 | | | | |
| $R_\tau$ | 20.84 ± 0.13 | .001 | −.001 | .113 | .033 | .051 | 1.00 | | | |
| $A^{0,{\rm e}}_{\rm FB}$ | 0.0171 ± 0.0049 | .057 | .001 | −.006 | −.106 | .000 | −.001 | 1.00 | | |
| $A^{0,\mu}_{\rm FB}$ | 0.0165 ± 0.0025 | .064 | .006 | −.002 | .025 | .008 | .000 | −.016 | 1.00 | |
| $A^{0,\tau}_{\rm FB}$ | 0.0241 ± 0.0037 | .043 | .003 | −.002 | .015 | .000 | .012 | −.015 | .014 | 1.00 |
| $\chi^2/N_{{\rm d}f}$ = 158/166 | | | | | L3 | | | | | |
| $m_{\rm Z}$ [GeV] | 91.1897 ± 0.0030 | 1.00 | | | | | | | | |
| $\Gamma_{\rm Z}$ [GeV] | 2.5025 ± 0.0041 | .065 | 1.00 | | | | | | | |
| $\sigma^0_{\rm h}$ [nb] | 41.535 ± 0.054 | .009 | −.343 | 1.00 | | | | | | |
| $R_{\rm e}$ | 20.815 ± 0.089 | .108 | −.007 | .075 | 1.00 | | | | | |
| $R_\mu$ | 20.861 ± 0.097 | −.001 | .002 | .077 | .030 | 1.00 | | | | |
| $R_\tau$ | 20.79 ± 0.13 | .002 | .005 | .053 | .024 | .020 | 1.00 | | | |
| $A^{0,{\rm e}}_{\rm FB}$ | 0.0107 ± 0.0058 | −.045 | .055 | −.006 | −.146 | −.001 | −.003 | 1.00 | | |
| $A^{0,\mu}_{\rm FB}$ | 0.0188 ± 0.0033 | .052 | .004 | .005 | .017 | .005 | .000 | .011 | 1.00 | |
| $A^{0,\tau}_{\rm FB}$ | 0.0260 ± 0.0047 | .034 | .004 | .003 | .012 | .000 | .007 | −.008 | .006 | 1.00 |
| $\chi^2/N_{{\rm d}f}$ = 155/194 | | | | | OPAL | | | | | |
| $m_{\rm Z}$ [GeV] | 91.1858 ± 0.0030 | 1.00 | | | | | | | | |
| $\Gamma_{\rm Z}$ [GeV] | 2.4948 ± 0.0041 | .049 | 1.00 | | | | | | | |
| $\sigma^0_{\rm h}$ [nb] | 41.501 ± 0.055 | .031 | −.352 | 1.00 | | | | | | |
| $R_{\rm e}$ | 20.901 ± 0.084 | .108 | .011 | .155 | 1.00 | | | | | |
| $R_\mu$ | 20.811 ± 0.058 | .001 | .020 | .222 | .093 | 1.00 | | | | |
| $R_\tau$ | 20.832 ± 0.091 | .001 | .013 | .137 | .039 | .051 | 1.00 | | | |
| $A^{0,{\rm e}}_{\rm FB}$ | 0.0089 ± 0.0045 | −.053 | −.005 | .011 | −.222 | −.001 | .005 | 1.00 | | |
| $A^{0,\mu}_{\rm FB}$ | 0.0159 ± 0.0023 | .077 | −.002 | .011 | .031 | .018 | .004 | −.012 | 1.00 | |
| $A^{0,\tau}_{\rm FB}$ | 0.0145 ± 0.0030 | .059 | −.003 | .003 | .015 | −.010 | .007 | −.010 | .013 | 1.00 |

Table 2: Line Shape and asymmetry parameters from fits to the data of the four LEP experiments and their correlation coefficients.

For completeness the partial decay widths of the Z boson are listed in Table 4, although they are more correlated than the ratios given in Table 3. The leptonic pole cross-section, $\sigma^0_\ell$, defined as

$$\sigma^0_\ell \equiv \frac{12\pi}{m^2_{\rm Z}} \frac{\Gamma^2_{\ell\ell}}{\Gamma^2_{\rm Z}} \,,$$

in analogy to $\sigma^0_{\rm h}$, is shown in the last line of the Table. Because QCD final state corrections appear

quadratically in the denominator via $\Gamma_{\rm Z}$, $\sigma^0_\ell$ has a higher sensitivity to $\alpha_s$ than $\sigma^0_{\rm h}$ or $R_\ell$, where the dependence on QCD corrections is only linear.

| without lepton universality | | correlations | | | | | | | | |
|---|---|---|---|---|---|---|---|---|---|---|
| $\chi^2/N_{\rm df}$ = 32.6/27 | | $m_{\rm Z}$ | $\Gamma_{\rm Z}$ | $\sigma^0_{\rm h}$ | $R_{\rm e}$ | $R_\mu$ | $R_\tau$ | $A^{0,{\rm e}}_{\rm FB}$ | $A^{0,\mu}_{\rm FB}$ | $A^{0,\tau}_{\rm FB}$ |
| $m_{\rm Z}$ [GeV] | 91.1876± 0.0021 | 1.00 | | | | | | | | |
| $\Gamma_{\rm Z}$ [GeV] | 2.4952 ± 0.0023 | −.024 | 1.00 | | | | | | | |
| $\sigma^0_{\rm h}$ [nb] | 41.541 ± 0.037 | −.044 | −.297 | 1.00 | | | | | | |
| $R_{\rm e}$ | 20.804 ± 0.050 | .078 | −.011 | .105 | 1.00 | | | | | |
| $R_\mu$ | 20.785 ± 0.033 | .000 | .008 | .131 | .069 | 1.00 | | | | |
| $R_\tau$ | 20.764 ± 0.045 | .002 | .006 | .092 | .046 | .069 | 1.00 | | | |
| $A^{0,{\rm e}}_{\rm FB}$ | 0.0145 ± 0.0025 | −.014 | .007 | .001 | −.371 | .001 | .003 | 1.00 | | |
| $A^{0,\mu}_{\rm FB}$ | 0.0169 ± 0.0013 | .046 | .002 | .003 | .020 | .012 | .001 | −.024 | 1.00 | |
| $A^{0,\tau}_{\rm FB}$ | 0.0188 ± 0.0017 | .035 | .001 | .002 | .013 | −.003 | .009 | −.020 | .046 | 1.00 |

with lepton universality

| $\chi^2/N_{\rm df}$ = 36.5/31 | | $m_{\rm Z}$ | $\Gamma_{\rm Z}$ | $\sigma^0_{\rm h}$ | $R_\ell$ | $A^{0,\ell}_{\rm FB}$ |
|---|---|---|---|---|---|---|
| $m_{\rm Z}$ [GeV] | 91.1875± 0.0021 | 1.00 | | | | |
| $\Gamma_{\rm Z}$ [GeV] | 2.4952 ± 0.0023 | −.023 | 1.00 | | | |
| $\sigma^0_{\rm h}$ [nb] | 41.540 ± 0.037 | −.045 | −.297 | 1.00 | | |
| $R_\ell$ | 20.767 ± 0.025 | .033 | .004 | .183 | 1.00 | |
| $A^{0,\ell}_{\rm FB}$ | 0.0171 ± 0.0010 | .055 | .003 | .006 | −.056 | 1.00 |

Table 3: Average line shape and asymmetry parameters from the data of the four LEP experiments, without and with the assumption of lepton universality.

| without lepton universality | | correlations | | | |
|---|---|---|---|---|---|
| $\Gamma_{\rm had}$ [MeV] | 1745.8 ±2.7 | 1.00 | | | |
| $\Gamma_{\rm ee}$ [MeV] | 83.92±0.12 | −0.29 | 1.00 | | |
| $\Gamma_{\mu\mu}$ [MeV] | 83.99±0.18 | 0.66 | −0.20 | 1.00 | |
| $\Gamma_{\tau\tau}$ [MeV] | 84.08±0.22 | 0.54 | −0.17 | 0.39 | 1.00 |

with lepton universality

| | | | | |
|---|---|---|---|---|
| $\Gamma_{\rm inv}$ [MeV] | 499.0 ±1.5 | 1.00 | | |
| $\Gamma_{\rm had}$ [MeV] | 1744.4 ±2.0 | −0.29 | 1.00 | |
| $\Gamma_{\ell\ell}$ [MeV] | 83.984±0.086 | 0.49 | 0.39 | 1.00 |
| $\Gamma_{\rm inv}/\Gamma_{\ell\ell}$ | 5.942 ±0.016 | | | |
| $\sigma^0_\ell$ [nb] | 2.0003±0.0027 | | | |

Table 4: Partial decay widths of the Z boson, derived from the results of the 9-parameter averages in Table 3. In the case of lepton universality, $\Gamma_{\ell\ell}$ refers to the partial Z width for the decay into a pair of massless charged leptons.

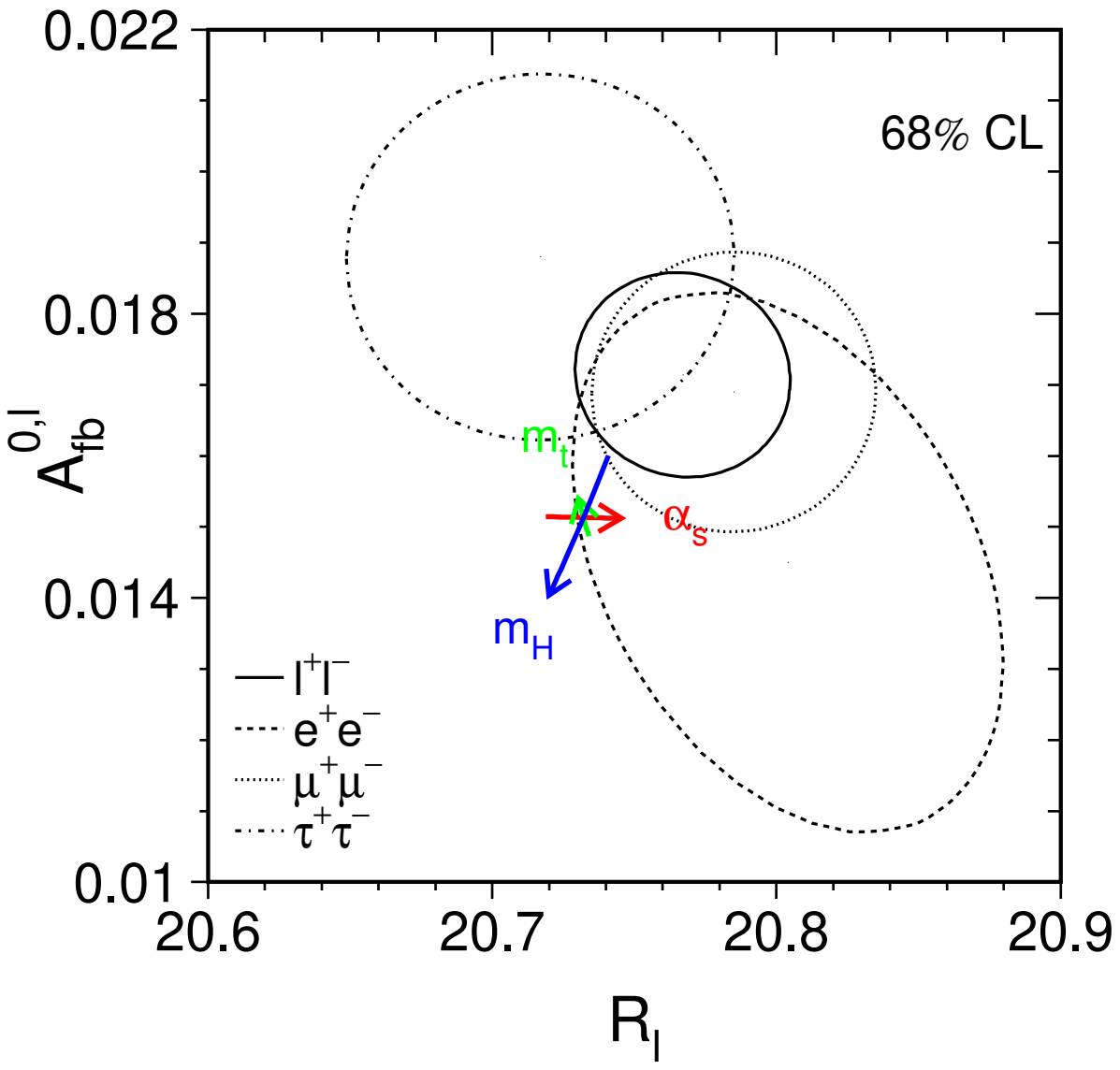


Figure 1: Contours of 68% probability in the $R_\ell$-$A_{\rm FB}^{0,\ell}$ plane. For better comparison the results for the $\tau$ lepton are corrected to correspond to the massless case. The Standard Model prediction for $m_{\rm Z} = 91.1875$ GeV, $m_{\rm t} = 174.3$ GeV, $m_{\rm H} = 300$ GeV, and $\alpha_{\rm s}(m_{\rm Z}^2) = 0.119$ is also shown. The lines with arrows correspond to the variation of the Standard Model prediction when $m_{\rm t}$, $m_{\rm H}$ and $\alpha_{\rm s}(m_{\rm Z}^2)$ are varied in the intervals $m_{\rm t} = 174.3 \pm 5.1$ GeV, $m_{\rm H} = 300^{+700}_{-187}$ GeV, and $\alpha_{\rm s}(m_{\rm Z}^2) = 0.119 \pm 0.002$, respectively. The arrows point in the direction of increasing values of $m_{\rm t}$, $m_{\rm H}$ and $\alpha_{\rm s}$.

# 3 The $\tau$ Polarisation

**Updates with respect to last summer:**
DELPHI have finalised their results.
OPAL have updated their results.

The longitudinal $\tau$ polarisation $\mathcal{P}_\tau$ of $\tau$ pairs produced in Z decays is defined as

$$\mathcal{P}_\tau \equiv \frac{\sigma_{\mathrm{R}} - \sigma_{\mathrm{L}}}{\sigma_{\mathrm{R}} + \sigma_{\mathrm{L}}}, \tag{5}$$

where $\sigma_{\mathrm{R}}$ and $\sigma_{\mathrm{L}}$ are the $\tau$-pair cross sections for the production of a right-handed and left-handed $\tau^-$, respectively. The distribution of $\mathcal{P}_\tau$ as a function of the polar scattering angle $\theta$ between the $\mathrm{e}^-$ and the $\tau^-$, at $\sqrt{s} = m_{\mathrm{Z}}$, is given by

$$\mathcal{P}_\tau(\cos\theta) = -\frac{\mathcal{A}_\tau(1+\cos^2\theta) + 2\mathcal{A}_{\mathrm{e}}\cos\theta}{1+\cos^2\theta + 2\mathcal{A}_\tau\mathcal{A}_{\mathrm{e}}\cos\theta}, \tag{6}$$

with $\mathcal{A}_{\mathrm{e}}$ and $\mathcal{A}_\tau$ as defined in Equation (4). Equation (6) is valid for pure Z exchange. The effects of $\gamma$ exchange, $\gamma$-Z interference and electromagnetic radiative corrections in the initial and final states are taken into account in the experimental analyses. In particular, these corrections account for the $\sqrt{s}$ dependence of the $\tau$ polarisation, which is important because the off-peak data are included in the event samples for all experiments. When averaged over all production angles $\mathcal{P}_\tau$ is a measurement of $\mathcal{A}_\tau$. As a function of $\cos\theta$, $\mathcal{P}_\tau(\cos\theta)$ provides nearly independent determinations of both $\mathcal{A}_\tau$ and $\mathcal{A}_{\mathrm{e}}$, thus allowing a test of the universality of the couplings of the Z to e and $\tau$.

Each experiment makes separate $\mathcal{P}_\tau$ measurements using the five $\tau$ decay modes $\mathrm{e}\nu\overline{\nu}$, $\mu\nu\overline{\nu}$, $\pi\nu$, $\rho\nu$ and $a_1\nu$ [16–19]. The $\rho\nu$ and $\pi\nu$ are the most sensitive channels, contributing weights of about 40% each in the average. DELPHI and L3 have also used an inclusive hadronic analysis. The combination is made using the results from each experiment already averaged over the $\tau$ decay modes.

## 3.1 Results

Tables 5 and 6 show the most recent results for $\mathcal{A}_\tau$ and $\mathcal{A}_{\mathrm{e}}$ obtained by the four LEP collaborations [16–19] and their combination. Common systematic errors arise from uncertainties in the decay radiation in the $\pi\nu$ and $\rho\nu$ channels, and in the modelling of the $a_1$ decays [20]. These errors need further investigation and might need to be taken into account for the final results (see Reference 18). For the current combination the systematic errors on $\mathcal{A}_\tau$ and $\mathcal{A}_{\mathrm{e}}$ are treated as uncorrelated between the experiments. The statistical correlation between the extracted values of $\mathcal{A}_\tau$ and $\mathcal{A}_{\mathrm{e}}$ is small ($\leq 5\%$), and is neglected.

The average values for $\mathcal{A}_\tau$ and $\mathcal{A}_{\mathrm{e}}$:

$$\mathcal{A}_\tau = 0.1439 \pm 0.0042 \tag{7}$$
$$\mathcal{A}_{\mathrm{e}} = 0.1498 \pm 0.0048, \tag{8}$$

are compatible, in agreement with lepton universality. Assuming e-$\tau$ universality, the values for $\mathcal{A}_\tau$ and $\mathcal{A}_{\mathrm{e}}$ can be combined. This combination is performed neglecting any possible common systematic error between $\mathcal{A}_\tau$ and $\mathcal{A}_{\mathrm{e}}$ within a given experiment, as these errors are also estimated to be small. The combined result of $\mathcal{A}_\tau$ and $\mathcal{A}_{\mathrm{e}}$ is:

$$\mathcal{A}_\ell = 0.1464 \pm 0.0032. \tag{9}$$

| Experiment | | $\mathcal{A}_\tau$ |
|---|---|---|
| ALEPH | (90 - 95), prel. | $0.1452 \pm 0.0052 \pm 0.0032$ |
| DELPHI | (90 - 95), final | $0.1359 \pm 0.0079 \pm 0.0055$ |
| L3 | (90 - 95), final | $0.1476 \pm 0.0088 \pm 0.0062$ |
| OPAL | (90 - 95), prel. | $0.1456 \pm 0.0075 \pm 0.0057$ |
| LEP Average | | $0.1439 \pm 0.0042$ |

Table 5: LEP results for $\mathcal{A}_\tau$. The $\chi^2$/d.o.f. for the average is 0.9/3. The first error is statistical and the second systematic. In the LEP average, statistical and systematic errors are combined in quadrature. The systematic component of the error is $\pm 0.0023$.

| Experiment | | $\mathcal{A}_\mathrm{e}$ |
|---|---|---|
| ALEPH | (90 - 95), prel. | $0.1505 \pm 0.0069 \pm 0.0010$ |
| DELPHI | (90 - 95), final | $0.1382 \pm 0.0116 \pm 0.0005$ |
| L3 | (90 - 95), final | $0.1678 \pm 0.0127 \pm 0.0030$ |
| OPAL | (90 - 95), prel. | $0.1456 \pm 0.0103 \pm 0.0034$ |
| LEP Average | | $0.1498 \pm 0.0048$ |

Table 6: LEP results for $\mathcal{A}_\mathrm{e}$. The $\chi^2$/d.o.f. for the average is 3.1/3. The first error is statistical and the second systematic. In the LEP average, statistical and systematic errors are combined in quadrature. The systematic component of the error is $\pm 0.0010$.

# 4 Measurement of $A_{\rm LR}$ at SLC

**Updates with respect to last summer:**
SLD have final results for $A_{\rm LR}$ and the leptonic left-right forward-backward asymmetries.

The measurement of the left-right cross section asymmetry ($A_{\rm LR}$) by SLD [21] at the SLC provides a systematically precise, statistics-dominated determination of the coupling $\mathcal{A}_{\rm e}$, and is presently the most precise single measurement, with the smallest systematic error, of this quantity. In principle the analysis is straightforward: one counts the numbers of Z bosons produced by left and right longitudinally polarised electrons, forms an asymmetry, and then divides by the luminosity-weighted $e^-$ beam polarisation magnitude (the $e^+$ beam is not polarised):

$$A_{\rm LR} = \frac{N_{\rm L} - N_{\rm R}}{N_{\rm L} + N_{\rm R}} \frac{1}{P_{\rm e}}. \tag{10}$$

Since the advent of high polarisation "strained lattice" GaAs photocathodes (1994), the average electron polarisation at the interaction point has been in the range 73% to 77%. The method requires no detailed final state event identification ($e^+e^-$ final state events are removed, as are non-Z backgrounds) and is insensitive to all acceptance and efficiency effects. The small total systematic error of 0.64% is dominated by the 0.50% systematic error in the determination of the $e^-$ polarisation. The statistical error on $A_{\rm LR}$ is about 1.3%.

The precision Compton polarimeter detects beam electrons that have been scattered by photons from a circularly polarised laser. Two additional polarimeters that are sensitive to the Compton-scattered photons and which are operated in the absence of positron beam, have verified the precision polarimeter result and are used to set a calibration uncertainty of 0.4%. In 1998, a dedicated experiment was performed in order to directly test the expectation that accidental polarisation of the positron beam was negligible; the $e^+$ polarisation was found to be consistent with zero $(-0.02\pm0.07)\%$.

The $A_{\rm LR}$ analysis includes several very small corrections. The polarimeter result is corrected for higher order QED and accelerator related effects, a total of $(-0.22 \pm 0.15)\%$ for 1997/98 data. The event asymmetry is corrected for backgrounds and accelerator asymmetries, a total of $(+0.15\pm0.07)\%$, for 1997/98 data.

The translation of the $A_{\rm LR}$ result to a "pole" value is a $(-2.5\pm0.4)\%$ effect, where the uncertainty arises from the precision of the centre-of-mass energy determination. This small error due to the beam energy measurement is slightly larger than seen previously (it was closer to 0.3%) and reflects the results of a scan of the Z peak used to calibrate the energy spectrometers to $m_{\rm Z}$ from LEP data, which was performed for the first time during the most recent SLC run. The pole value, $A^0_{\rm LR}$, is equivalent to a measurement of $\mathcal{A}_{\rm e}$.

The 2000 result is included in a running average of all of the SLD $A_{\rm LR}$ measurements (1992, 1993, 1994/1995, 1996, 1997 and 1998). This updated result for $A^0_{\rm LR}$ ($\mathcal{A}_{\rm e}$) is $0.1514\pm0.0022$. In addition, the left-right forward-backward asymmetries for leptonic final states are measured [22]. From these, the parameters $\mathcal{A}_{\rm e}$, $\mathcal{A}_\mu$ and $\mathcal{A}_\tau$ can be determined. The results are $\mathcal{A}_{\rm e} = 0.1544\pm0.0060$, $\mathcal{A}_\mu = 0.142\pm0.015$ and $\mathcal{A}_\tau = 0.136 \pm 0.015$. The lepton-based result for $\mathcal{A}_{\rm e}$ can be combined with the $A^0_{\rm LR}$ result to yield $\mathcal{A}_{\rm e} = 0.1516 \pm 0.0021$, including small correlations in the systematic errors. The correlation of this measurement with $\mathcal{A}_\mu$ and $\mathcal{A}_\tau$ is indicated in Table 7.

Assuming lepton universality, the $A_{\rm LR}$ result and the results on the leptonic left-right forward-backward asymmetries can be combined, while accounting for small correlated systematic errors,

yielding

$$\mathcal{A}_\ell = 0.1513 \pm 0.0021. \tag{11}$$

| | $\mathcal{A}_\mathrm{e}$ | $\mathcal{A}_\mu$ | $\mathcal{A}_\tau$ |
|---|---|---|---|
| $\mathcal{A}_\mathrm{e}$ | 1.000 | | |
| $\mathcal{A}_\mu$ | 0.038 | 1.000 | |
| $\mathcal{A}_\tau$ | 0.033 | 0.007 | 1.000 |

Table 7: Correlation coefficients between $\mathcal{A}_\mathrm{e}$, $\mathcal{A}_\mu$ and $\mathcal{A}_\tau$

# 5 Results from b and c Quarks

**Updates with respect to last summer:**
DELPHI has presented new measurements of $A_{\rm FB}^{\rm b\bar{b}}$ and $A_{\rm FB}^{\rm c\bar{c}}$.
SLD has presented updated measurements of $R_{\rm b}$, $R_{\rm c}$, $\mathcal{A}_{\rm b}$ with leptons and vertex charge and $\mathcal{A}_{\rm c}$ with leptons and D-mesons.
ALEPH has presented a new measurement of BR($\rm b \to \ell$) and BR($\rm b \to c \to \bar{\ell}$) and L3 has published their measurement of $R_{\rm b}$ and BR($\rm b \to \ell$).

The relevant quantities in the heavy quark sector at LEP/SLD which are currently determined by the combination procedure are:

- The ratios of the b and c quark partial widths of the Z to its total hadronic partial width: $R_{\rm b}^0 \equiv \Gamma_{\rm b\bar{b}}/\Gamma_{\rm had}$ and $R_{\rm c}^0 \equiv \Gamma_{\rm c\bar{c}}/\Gamma_{\rm had}$.
- The forward-backward asymmetries, $A_{\rm FB}^{\rm b\bar{b}}$ and $A_{\rm FB}^{\rm c\bar{c}}$.
- The final state coupling parameters $\mathcal{A}_{\rm b}$, $\mathcal{A}_{\rm c}$ obtained from the left-right-forward-backward asymmetry at SLD.
- The semileptonic branching ratios, BR($\rm b \to \ell$), BR($\rm b \to c \to \bar{\ell}$) and BR($\rm c \to \ell$), and the average time-integrated $\rm B^0\overline{B^0}$ mixing parameter, $\overline{\chi}$. These are often determined at the same time or with similar methods as the asymmetries. Including them in the combination greatly reduces the errors. For example the measurements of $\overline{\chi}$ act as an effective measurement of the charge tagging efficiency, so that all errors coming from the mixture of different lepton sources in $\rm b\overline{b}$ events cancel in the asymmetries.
- The probability that a c quark produces a $\rm D^+$, $\rm D_s$, $\rm D^{*+}$ meson[2] or a charmed baryon. The probability that a c quark fragments into a $\rm D^0$ is calculated from the constraint that the probabilities for the weakly decaying charmed hadrons add up to one.

A full description of the averaging procedure is published in [3]; the main motivations for the procedure are outlined here. Several analyses measure more than one parameter simultaneously, for example the asymmetry measurements with leptons or D mesons. Some of the measurements of electroweak parameters depend explicitly on the values of other parameters, for example $R_{\rm b}$ depends on $R_{\rm c}$. The common tagging and analysis techniques lead to common sources of systematic uncertainty, in particular for the double-tag measurements of $R_{\rm b}$. The starting point for the combination is to ensure that all the analyses use a common set of assumptions for input parameters which give rise to systematic uncertainties. The input parameters are updated and extended [1, 23] to accommodate new analyses and more recent measurements. The correlations and interdependences of the input measurements are then taken into account in a $\chi^2$ minimisation which results in the combined electroweak parameters and their correlation matrix.

In a first fit the asymmetry measurements on peak, above peak and below peak are corrected to three common centre-of-mass energies and are then combined at each energy point. The results of this fit, including the SLD results, are given in Appendix A. The dependence of the average asymmetries on centre-of-mass energy agrees with the prediction of the Standard Model. A second fit is made to derive the pole asymmetries $A_{\rm FB}^{0,\rm q}$ from the measured quark asymmetries, in which all the off-peak

[2] Actually the product $\rm P(c \to D^{*+}) \times BR(D^{*+} \to \pi^+ D^0)$ is fitted because this quantity is needed and measured by the LEP experiments.

asymmetry measurements are corrected to the peak energy before combining. This fit determines a total of 14 parameters: the two partial widths, two LEP asymmetries, two coupling parameters from SLD, three semileptonic branching ratios, the average mixing parameter and the probabilities for c quark to fragment into a $D^+$, a $D_s$, a $D^{*+}$, or a charmed baryon. If the SLD measurements are excluded from the fit there are 12 parameters to be determined.

## 5.1 Summary of Measurements and Averaging Procedure

All measurements are presented by the LEP and SLD collaborations in a consistent manner for the purpose of combination. The tables prepared by the experiments include a detailed breakdown of the systematic error of each measurement and its dependence on other electroweak parameters. Where necessary, the experiments apply small corrections to their results in order to use agreed values and ranges for the input parameters to calculate systematic errors. The measurements, corrected where necessary, are summarised in Appendix A in Tables 44–63, where the statistical and systematic errors are quoted separately. The correlated systematic entries are from physics sources shared with one or more other results in the table and are derived from the full breakdown of common systematic uncertainties. The uncorrelated systematic entries come from the remaining sources.

### 5.1.1 Averaging Procedure

A $\chi^2$ minimisation procedure is used to derive the values of the heavy-flavour electroweak parameters as published in Reference 3. The full statistical and systematic covariance matrix for all measurements is calculated. This correlation matrix takes into account correlations between different measurements of one experiment and between different experiments. The explicit dependence of each measurement on the other parameters is also accounted for.

Since c-quark events form the main background in the $R_b$ analyses, in the lifetime $R_b$ analyses, the value of $R_b$ depends on the value of $R_c$. If $R_b$ and $R_c$ are measured in the same analysis, this is reflected in the correlation matrix for the results. However the analyses do not determine $R_b$ and $R_c$ simultaneously but instead measure $R_b$ for an assumed value of $R_c$. In this case the dependence is parameterised as

$$R_b \;=\; R_b^{\rm meas} + a(R_c)\frac{(R_c - R_c^{\rm used})}{R_c}. \qquad (12)$$

In this expression, $R_b^{\rm meas}$ is the result of the analysis assuming a value of $R_c = R_c^{\rm used}$. The values of $R_c^{\rm used}$ and the coefficients $a(R_c)$ are given in Table 44 where appropriate. The dependence of all other measurements on other electroweak parameters is treated in the same way, with coefficients $a(x)$ describing the dependence on parameter $x$.

### 5.1.2 Partial Width Measurements

The measurements of $R_b$ and $R_c$ fall into two categories. In the first, called a single-tag measurement, a method to select b or c events is devised, and the number of tagged events is counted. This number must then be corrected for backgrounds from other flavours and for the tagging efficiency to calculate the true fraction of hadronic Z decays of that flavour. The dominant systematic errors come from understanding the branching ratios and detection efficiencies which give the overall tagging efficiency.

For the second technique, called a double-tag measurement, each event is divided into two hemispheres. With $N_t$ being the number of tagged hemispheres, $N_{tt}$ the number of events with both hemispheres tagged and $N_{\rm had}$ the total number of hadronic Z decays one has

$$\frac{N_t}{2N_{\rm had}} = \varepsilon_{\rm b}R_{\rm b} + \varepsilon_{\rm c}R_{\rm c} + \varepsilon_{\rm uds}(1 - R_{\rm b} - R_{\rm c}), \tag{13}$$

$$\frac{N_{tt}}{N_{\rm had}} = \mathcal{C}_{\rm b}\varepsilon_{\rm b}^2R_{\rm b} + \mathcal{C}_{\rm c}\varepsilon_{\rm c}^2R_{\rm c} + \mathcal{C}_{\rm uds}\varepsilon_{\rm uds}^2(1 - R_{\rm b} - R_{\rm c}), \tag{14}$$

where $\varepsilon_{\rm b}$, $\varepsilon_{\rm c}$ and $\varepsilon_{\rm uds}$ are the tagging efficiencies per hemisphere for b, c and light-quark events, and $\mathcal{C}_{\rm q} \neq 1$ accounts for the fact that the tagging efficiencies between the hemispheres may be correlated. In the case of $R_{\rm b}$ one has $\varepsilon_{\rm b} \gg \varepsilon_{\rm c} \gg \varepsilon_{\rm uds}$, $\mathcal{C}_{\rm b} \approx 1$. The correlations for the other flavours can be neglected. These equations can be solved to give $R_{\rm b}$ and $\varepsilon_{\rm b}$. Neglecting the c and uds backgrounds and the correlations they are approximately given by

$$\varepsilon_{\rm b} \approx 2N_{tt}/N_t, \tag{15}$$

$$R_{\rm b} \approx N_t^2/(4N_{tt}N_{\rm had}). \tag{16}$$

The double-tagging method has the advantage that the b tagging efficiency is derived from the data, reducing the systematic error. The residual background of other flavours in the sample, and the evaluation of the correlation between the tagging efficiencies in the two hemispheres of the event are the main sources of systematic uncertainty in such an analysis.

This method can be enhanced by including more tags. All additional efficiencies can be determined from the data, reducing the statistical uncertainties without adding new systematic uncertainties.

Small corrections must be applied to the results to obtain the partial width ratios $R_{\rm b}^0$ and $R_{\rm c}^0$ from the cross section ratios $R_{\rm b}$ and $R_{\rm c}$. These corrections depend slightly on the invariant mass cutoff of the simulations used by the experiments, so that they are applied by the collaborations before the combination.

The partial width measurements included are:

- Lifetime (and lepton) double tag measurements for $R_{\rm b}$ from ALEPH [24], DELPHI [25], L3 [26], OPAL [27] and SLD [28]. These are the most precise determinations of $R_{\rm b}$. Since they completely dominate the combined result, no other $R_{\rm b}$ measurements are used at present. The basic features of the double-tag technique are discussed above. In the ALEPH, DELPHI, OPAL and SLD measurements the charm rejection is enhanced by using the invariant mass information. DELPHI, OPAL and SLD also add kinematic information from the particles at the secondary vertex. The ALEPH and DELPHI measurements make use of several different tags; this improves the statistical accuracy and reduces the systematic errors due to hemisphere correlations and charm contamination, compared with the simple single/double tag.
- Analyses with $\rm D/D^{*\pm}$ mesons to measure $R_{\rm c}$ from ALEPH, DELPHI and OPAL. All measurements are constructed in such a way that no assumptions on the energy dependence of charm fragmentation are necessary. The available measurements can be divided into four groups:
  - inclusive/exclusive double tag (ALEPH [29], DELPHI [30, 31], OPAL [32]): In a first step $\rm D^{*\pm}$ mesons are reconstructed in several decay channels and their production rate is measured, which depends on the product $R_{\rm c} \times {\rm P(c \to D^{*+}) \times BR(D^{*+} \to \pi^+ D^0)}$. This sample of $\rm c\overline{c}$ (and $\rm b\overline{b}$) events is then used to measure $\rm P(c \to D^{*+}) \times BR(D^{*+} \to \pi^+ D^0)$ using a slow pion tag in the opposite hemisphere. In the ALEPH measurement $R_{\rm c}$ is unfolded internally in the analysis so that no explicit $\rm P(c \to D^{*+}) \times BR(D^{*+} \to \pi^+ D^0)$ is available.

  - exclusive double tag (ALEPH [29]): This analysis uses exclusively reconstructed $D^{*+}$, $D^0$ and $D^+$ mesons in different decay channels. It has lower statistics but better purity than the inclusive analyses.
  - reconstruction of all weakly decaying charmed states (ALEPH [33], DELPHI [31], OPAL [34]): These analyses make the assumption that the production rates of $D^0$, $D^+$, $D_s$ and $\Lambda_c$ in $c\overline{c}$ events add up to one with small corrections due to unmeasured charms strange baryons. This is a single tag measurement, relying only on knowing the decay branching ratios of the charm hadrons. These analyses are also used to measure the c hadron production ratios which are needed for the $R_b$ analyses.

- A lifetime plus mass double tag from SLD to measure $R_c$ [28]. This analysis uses the same tagging algorithm as the SLD $R_b$ analysis, but with the neural net tuned to tag charm. Although the charm tag has a purity of about 84%, most of the background is from b which can be measured with high precision from the b/c mixed tag rate.

- A measurement of $R_c$ using single leptons assuming $BR(c \to \ell)$ from ALEPH [29].

To avoid effects from non linearities in the fit, for the inclusive/exclusive single/double tag and for the charm-counting analyses, the products $R_cP(c \to D^{*+}) \times BR(D^{*+} \to \pi^+ D^0)$, $R_cf_{D^0}$, $R_cf_{D^+}$, $R_cf_{D_s}$ and $R_cf_{\Lambda_c}$that are actually measured in the analyses are directly used as inputs to the fit. The measurements of the production rates of weakly decaying charmed hadrons, especially $R_cf_{D_s}$ and $R_cf_{\Lambda_c}$ have a substantial error due to the branching ratio of the decay mode used. Since this error is a relative one there is a potential bias towards lower measurements. To avoid this bias, for the production rates of weakly decaying charmed hadrons the logarithm of the production rates instead of the rates themselves are input to the fit. For $R_cf_{D^0}$ and $R_cf_{D^+}$ the difference between the results using the logarithm or the value itself is negligible. For $R_cf_{D_s}$ and $R_cf_{\Lambda_c}$ the difference in the $R_c$-result is about one tenth of a standard deviation.

### 5.1.3 Asymmetry Measurements

All b and c asymmetries given by the experiments are corrected to full acceptance.

The QCD corrections to the forward-backward asymmetries depend strongly on the experimental analyses. For this reason the numbers given by the collaborations are also corrected for QCD effects. A detailed description of the procedure can be found in [35] with updates reported in [1]

For the 12- and 14-parameter fits described above, the LEP peak and off-peak asymmetries are corrected to $\sqrt{s} = 91.26$ GeV using the predicted dependence from ZFITTER [36]. The slope of the asymmetry around $m_Z$ depends only on the axial coupling and the charge of the initial and final state fermions and is thus independent of the value of the asymmetry itself.

After calculating the overall averages, the quark pole asymmetries, $A_{FB}^{0,q}$, are derived by applying the corrections described below. To relate the pole asymmetries to the measured ones a few corrections that are summarised in Table 8 have to be applied. These corrections are due to the energy shift from 91.26 GeV to $m_Z$, initial state radiation, $\gamma$ exchange and $\gamma$-Z interference. A very small correction due to the nonzero value of the b quark mass is included in the correction called $\gamma$-Z interference. All corrections are calculated using ZFITTER.

The SLD left-right-forward-backward asymmetries are also corrected for all radiative effects and are directly presented in terms of $\mathcal{A}_b$ and $\mathcal{A}_c$.

| Source | $\delta A_{\rm FB}^{\rm b}$ | $\delta A_{\rm FB}^{\rm c}$ |
|---|---|---|
| $\sqrt{s} = m_{\rm Z}$ | $-0.0013$ | $-0.0034$ |
| QED corrections | $+0.0041$ | $+0.0104$ |
| $\gamma$, $\gamma$-Z, mass | $-0.0003$ | $-0.0008$ |
| Total | $+0.0025$ | $+0.0062$ |

Table 8: Corrections to be applied to the quark asymmetries as $A_{\rm FB}^0 = A_{\rm FB}^{\rm meas} + \delta A_{\rm FB}$.

The measurements used are:

- Measurements of $A_{\rm FB}^{\rm b\bar{b}}$ and $A_{\rm FB}^{\rm c\bar{c}}$ using leptons from ALEPH [37], DELPHI [38], L3 [39] and OPAL [40]. These analyses measure either $A_{\rm FB}^{\rm b\bar{b}}$ only from a high $p_t$ lepton sample or they obtain $A_{\rm FB}^{\rm b\bar{b}}$ and $A_{\rm FB}^{\rm c\bar{c}}$ from a fit to the lepton spectra. In the case of OPAL the lepton information is combined with hadronic variables in a neural net. DELPHI uses in addition lifetime information and jet-charge in the hemisphere opposite to the lepton to separate the different lepton sources. Some asymmetry analyses also measure $\overline{\chi}$.
- Measurements of $A_{\rm FB}^{\rm b\bar{b}}$ based on lifetime tagged events with a hemisphere charge measurement from ALEPH [41], DELPHI [42], L3 [43] and OPAL [44]. These measurements contribute roughly the same weight to the combined result as the lepton fits.
- Analyses with D mesons to measure $A_{\rm FB}^{\rm c\bar{c}}$ from ALEPH [45] or $A_{\rm FB}^{\rm c\bar{c}}$ and $A_{\rm FB}^{\rm b\bar{b}}$ from DELPHI [46] and OPAL [47].
- Measurements of $\mathcal{A}_{\rm b}$ and $\mathcal{A}_{\rm c}$ from SLD. These results include measurements using lepton [48,49], D meson [50] and vertex mass plus hemisphere charge [51] tags, which have similar sources of systematic errors as the LEP asymmetry measurements. SLD also uses vertex mass for bottom or charm tag in conjunction with a kaon tag or a vertex charge tag for both $\mathcal{A}_{\rm b}$ and $\mathcal{A}_{\rm c}$ measurements [52–54].

#### 5.1.4 Other Measurements

The measurements of the charmed hadron fractions $\mathrm{P(c \to D^{*+}) \times BR(D^{*+} \to \pi^+ D^0)}$, $f(\mathrm{D^+})$, $f(\mathrm{D_s})$ and $f(\mathrm{c_{baryon}})$ are included in the $R_{\rm c}$ measurements and are described there.

ALEPH [55], DELPHI [56], L3 [26, 57] and OPAL [58] measure $\mathrm{BR(b \to \ell)}$, $\mathrm{BR(b \to c \to \bar{\ell})}$ and $\overline{\chi}$ or a subset of them from a sample of leptons opposite to a b-tagged hemisphere and from a double lepton sample. DELPHI [30] and OPAL [59] measure $\mathrm{BR(c \to \ell)}$ from a sample opposite to a high energy $\mathrm{D^{*\pm}}$.

### 5.2 Results

#### 5.2.1 Results of the 12-Parameter Fit to the LEP Data

Using the full averaging procedure gives the following combined results for the electroweak parameters:

$$R_{\rm b}^0 \quad = \quad 0.21648 \pm 0.00075 \tag{17}$$

$$
\begin{aligned}
R_{\rm c}^0 &= 0.1674 \pm 0.0047 \\
A_{\rm FB}^{0,\,{\rm b}} &= 0.0989 \pm 0.0020 \\
A_{\rm FB}^{0,\,{\rm c}} &= 0.0688 \pm 0.0035\,,
\end{aligned}
$$

where all corrections to the asymmetries and partial widths are applied. The $\chi^2$/d.o.f. is $49/(89-12)$. The corresponding correlation matrix is given in Table 9.

| | $R_{\rm b}^0$ | $R_{\rm c}^0$ | $A_{\rm FB}^{0,\,{\rm b}}$ | $A_{\rm FB}^{0,\,{\rm c}}$ |
|---|---|---|---|---|
| $R_{\rm b}^0$ | 1.00 | −0.15 | −0.03 | 0.01 |
| $R_{\rm c}^0$ | −0.15 | 1.00 | 0.07 | −0.01 |
| $A_{\rm FB}^{0,\,{\rm b}}$ | −0.03 | 0.07 | 1.00 | 0.11 |
| $A_{\rm FB}^{0,\,{\rm c}}$ | 0.01 | −0.01 | 0.11 | 1.00 |

Table 9: The correlation matrix for the four electroweak parameters from the 12-parameter fit.

### 5.2.2 Results of the 14-Parameter Fit to LEP and SLD Data

Including the SLD results for $R_{\rm b}$, $R_{\rm c}$, $\mathcal{A}_{\rm b}$ and $\mathcal{A}_{\rm c}$ into the fit the following results are obtained:

$$
\begin{aligned}
R_{\rm b}^0 &= 0.21653 \pm 0.00069 \\
R_{\rm c}^0 &= 0.1709 \pm 0.0034 \\
A_{\rm FB}^{0,\,{\rm b}} &= 0.0990 \pm 0.0020 \\
A_{\rm FB}^{0,\,{\rm c}} &= 0.0689 \pm 0.0035 \\
\mathcal{A}_{\rm b} &= 0.922 \pm 0.023 \\
\mathcal{A}_{\rm c} &= 0.631 \pm 0.026\,,
\end{aligned}
\tag{18}
$$

with a $\chi^2$/d.o.f. of $54/(98-14)$. The corresponding correlation matrix is given in Table 10 and the largest errors for the electroweak parameters are listed in Table 11.

In deriving these results the parameters $\mathcal{A}_{\rm b}$ and $\mathcal{A}_{\rm c}$ are treated as independent of the forward-backward asymmetries $A_{\rm FB}^{0,\,{\rm b}}$ and $A_{\rm FB}^{0,\,{\rm c}}$. In Figure 2 the results for $R_{\rm b}^0$ and $R_{\rm c}^0$ are shown compared with the Standard Model expectation.

| | $R_{\rm b}^0$ | $R_{\rm c}^0$ | $A_{\rm FB}^{0,\,{\rm b}}$ | $A_{\rm FB}^{0,\,{\rm c}}$ | $\mathcal{A}_{\rm b}$ | $\mathcal{A}_{\rm c}$ |
|---|---|---|---|---|---|---|
| $R_{\rm b}^0$ | 1.00 | −0.13 | −0.02 | 0.01 | −0.04 | 0.02 |
| $R_{\rm c}^0$ | −0.13 | 1.00 | 0.05 | −0.01 | 0.02 | −0.02 |
| $A_{\rm FB}^{0,\,{\rm b}}$ | −0.02 | 0.05 | 1.00 | 0.10 | 0.02 | 0.00 |
| $A_{\rm FB}^{0,\,{\rm c}}$ | 0.01 | −0.01 | 0.10 | 1.00 | 0.00 | 0.01 |
| $\mathcal{A}_{\rm b}$ | −0.04 | 0.02 | 0.02 | 0.00 | 1.00 | 0.14 |
| $\mathcal{A}_{\rm c}$ | 0.02 | −0.02 | 0.00 | 0.01 | 0.14 | 1.00 |

Table 10: The correlation matrix for the six electroweak parameters from the 14-parameter fit.

The 14 parameter fit yields the $\rm b \to \ell$ branching ratio:

$$
{\rm BR(b} \to \ell) \;=\; 0.1057 \pm 0.0019. \tag{19}
$$

| | $R_{\rm b}^0$ ($10^{-3}$) | $R_{\rm c}^0$ ($10^{-3}$) | $A_{\rm FB}^{0,\,\rm b}$ ($10^{-3}$) | $A_{\rm FB}^{0,\,\rm c}$ ($10^{-3}$) | $\mathcal{A}_{\rm b}$ ($10^{-2}$) | $\mathcal{A}_{\rm c}$ ($10^{-2}$) |
|---|---|---|---|---|---|---|
| statistics | 0.43 | 2.6 | 1.7 | 3.0 | 1.6 | 2.0 |
| internal systematics | 0.31 | 1.8 | 0.7 | 1.4 | 1.6 | 1.6 |
| QCD effects | 0.19 | 0.1 | 0.2 | 0.1 | 0.6 | 0.3 |
| BR(D $\rightarrow$ neut.) | 0.14 | 0.1 | 0 | 0 | 0 | 0 |
| D decay multiplicity | 0.12 | 0.2 | 0 | 0 | 0 | 0 |
| BR($\rm D^+ \rightarrow K^-\pi^+\pi^+$) | 0.10 | 0.3 | 0.1 | 0 | 0 | 0 |
| BR($\rm D_s \rightarrow \phi\pi^+$) | 0.02 | 0.7 | 0.1 | 0 | 0 | 0 |
| BR($\Lambda_{\rm c} \rightarrow$p $\rm K^-\pi^+$) | 0.06 | 0.6 | 0 | 0.1 | 0 | 0 |
| D lifetimes | 0.06 | 0.1 | 0 | 0.1 | 0 | 0 |
| gluon splitting | 0.26 | 0.6 | 0 | 0.2 | 0.1 | 0.1 |
| c fragmentation | 0.10 | 0.3 | 0.1 | 0.2 | 0.1 | 0.1 |
| light quarks | 0.07 | 0.3 | 0.5 | 0.1 | 0 | 0 |
| total | 0.69 | 3.4 | 2.0 | 3.5 | 2.3 | 2.6 |

Table 11: The dominant error sources for the electroweak parameters from the 14-parameter fit.

The largest error sources on this quantity are the dependences on the semileptonic decay models $\rm b \rightarrow \ell$, $\rm c \rightarrow \ell$ with

$$\begin{aligned} \Delta{\rm BR}({\rm b} \rightarrow \ell)|_{({\rm b}\rightarrow\ell){\rm model}} &= 0.0008, \\ \Delta{\rm BR}({\rm b} \rightarrow \ell)|_{({\rm c}\rightarrow\ell){\rm model}} &= 0.0005. \end{aligned}$$

Extensive studies are made to understand the size of these errors. If all the asymmetry measurements are excluded from the fit a consistent result is obtained with modelling errors of 0.0010 and 0.0006. The reduction of the modelling uncertainty is due to the inclusion of asymmetry measurements using different methods. Those using leptons depend on the semileptonic decay models while those using a lifetime tag and jet charge or D mesons do not. The mutual consistency of the asymmetry measurements effectively constrains the semileptonic decay models, and reduces the uncertainty in the semileptonic branching ratio.

The result of the full fit to the LEP+SLC results including the off-peak asymmetries and the non-electroweak parameters can be found in Appendix A. Results for the non-electroweak parameters are independent of the treatment of the off-peak asymmetries and the SLD data.

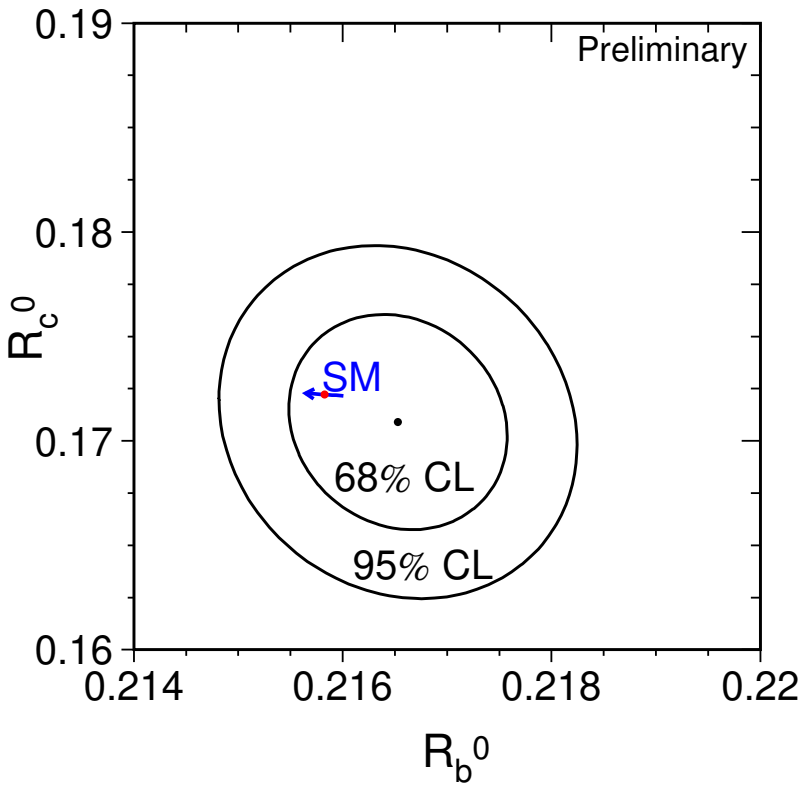


Figure 2: Contours in the $R_{\rm b}^0$-$R_{\rm c}^0$ plane derived from the LEP+SLD data, corresponding to 68% and 95% confidence levels assuming Gaussian systematic errors. The Standard Model prediction for $m_{\rm t} = 174.3 \pm 5.1$ GeV is also shown. The arrow points in the direction of increasing values of $m_{\rm t}$.

# 6 The Hadronic Charge Asymmetry $\langle Q_{\rm FB} \rangle$

**Updates with respect to last summer:**
L3 have published their result.

The LEP experiments ALEPH [60–62], DELPHI [63, 64], L3 [43] and OPAL [65, 66] have provided measurements of the hadronic charge asymmetry based on the mean difference in jet charges measured in the forward and backward event hemispheres, $\langle Q_{\rm FB} \rangle$. DELPHI have also provided a related measurement of the total charge asymmetry by making a charge assignment on an event-by-event basis and performing a likelihood fit [63]. The experimental values quoted for the average forward-backward charge difference, $\langle Q_{\rm FB} \rangle$, cannot be directly compared as some of them include detector dependent effects such as acceptances and efficiencies. Therefore the effective electroweak mixing angle, $\sin^2\theta^{\rm lept}_{\rm eff}$, as defined in Section 12.4, is used as a means of combining the experimental results summarised in Table 12.

| Experiment | | $\sin^2\theta^{\rm lept}_{\rm eff}$ |
|---|---|---|
| ALEPH | (90-94), final | $0.2322 \pm 0.0008 \pm 0.0011$ |
| DELPHI | (91-94), prel. | $0.2311 \pm 0.0010 \pm 0.0014$ |
| L3 | (91-95), final | $0.2327 \pm 0.0012 \pm 0.0013$ |
| OPAL | (91-94), prel. | $0.2326 \pm 0.0012 \pm 0.0013$ |
| LEP Average | | $0.2321 \pm 0.0010$ |

Table 12: Summary of the determination of $\sin^2\theta^{\rm lept}_{\rm eff}$ from inclusive hadronic charge asymmetries at LEP. For each experiment, the first error is statistical and the second systematic. The latter is dominated by fragmentation and decay modelling uncertainties.

The dominant source of systematic error arises from the modelling of the charge flow in the fragmentation process for each flavour. All experiments measure the required charge properties for $Z \to b\overline{b}$ events from the data. ALEPH also determines the charm charge properties from the data. The fragmentation model implemented in the JETSET Monte Carlo program [67] is used by all experiments as reference; the one of the HERWIG Monte Carlo program [68] is used for comparison. The JETSET fragmentation parameters are varied to estimate the systematic errors. The central values chosen by the experiments for these parameters are, however, not the same. The smaller of the two fragmentation errors in any pair of results is treated as common to both. The present average of $\sin^2\theta^{\rm lept}_{\rm eff}$ from $\langle Q_{\rm FB} \rangle$ and its associated error are not very sensitive to the treatment of common uncertainties. The ambiguities due to QCD corrections may cause changes in the derived value of $\sin^2\theta^{\rm lept}_{\rm eff}$. These are, however, well below the fragmentation uncertainties and experimental errors. The effect of fully correlating the estimated systematic uncertainties from this source between the experiments has a negligible effect upon the average and its error.

There is also some correlation between these results and those for $A^{b\bar{b}}_{\rm FB}$ using jet charges. The dominant source of correlation is again through uncertainties in the fragmentation and decay models used. The typical correlation between the derived values of $\sin^2\theta^{\rm lept}_{\rm eff}$ from the $\langle Q_{\rm FB} \rangle$ and the $A^{b\bar{b}}_{\rm FB}$ jet charge measurements is estimated to be about 20% to 25%. This leads to only a small change in the relative weights for the $A^{b\bar{b}}_{\rm FB}$ and $\langle Q_{\rm FB} \rangle$ results when averaging their $\sin^2\theta^{\rm lept}_{\rm eff}$ values (Section 12.4). Furthermore, the jet charge method contributes at most half of the weight of the $A^{b\bar{b}}_{\rm FB}$ measurement. Thus, the correlation between $\langle Q_{\rm FB} \rangle$ and $A^{b\bar{b}}_{\rm FB}$ from jet charge will have little impact on the overall Standard Model fit, and is neglected at present.

# 7 Averages for $f\bar{f}$ Production at LEP-II

**Updates with respect to last summer:**
Results are updated with data taken in 1999 and 2000.

Since the start of the LEP-II program LEP has delivered collisions at energies from $\sim 130$ GeV to $\sim 209$ GeV. The four LEP experiments have made measurements on the $e^+e^- \to f\bar{f}$ process over this range of energies, and preliminary combinations of these data are discussed in this note.

For the combination presented here, only data taken up to the end of June 2000 are considered. The nominal and actual centre-of-mass energies to which the LEP data are averaged for each year are given in Table 13.

A number of measurements on the process $e^+e^- \to f\bar{f}$ exist and are combined.

- preliminary averages of cross section and forward-backward asymmetry measurements
- a preliminary average of the differential cross section measurements, $\frac{d\sigma}{d\cos\theta}$, for the channels $e^+e^- \to \mu^+\mu^-$ and $e^+e^- \to \tau^+\tau^-$
- heavy flavour results $R_b$, $R_c$, $A_{FB}^{b\bar{b}}$ and $A_{FB}^{c\bar{c}}$

Complete results of the combinations are available on the web page [69] and are discussed in [70].

The combined results are interpreted in terms of contact interactions, the exchange of Z′ bosons, and contours of the S-Matrix parameters $j_{b,c}^{tot}$ and $j_{b,c}^{fb}$, that describe $\gamma$-Z interference, are derived. The interpretations are discussed fully in [70].

## 7.1 Cross Sections and Asymmetry Measurements

Cross section results are combined for the $e^+e^- \to q\bar{q}$, $e^+e^- \to \mu^+\mu^-$ and $e^+e^- \to \tau^+\tau^-$ channels, forward-backward asymmetry measurements are combined for the $\mu^+\mu^-$ and $\tau^+\tau^-$ final states. The averages are made for the samples of events with high $\sqrt{s'}$.

As before [71], the averaged results are given for two signal definitions:

- **Definition 1:** $\sqrt{s'}$ is taken to be the mass of the $s$-channel propagator, with the $f\bar{f}$ signal being defined by the cut $\sqrt{s'/s} > 0.85$. ISR-FSR photon interference is subtracted to render the propagator mass unambiguous.

- **Definition 2:** For dilepton events, $\sqrt{s'}$ is taken to be the bare invariant mass of the outgoing difermion pair. For hadronic events, it is taken to be the mass of the $s$-channel propagator. In both cases, ISR-FSR photon interference is included and the signal is defined by the cut $\sqrt{s'/s} > 0.85$. When calculating the contribution to the hadronic cross section due to ISR-FSR interference, since the propagator mass is ill-defined, it is replaced by the bare $q\bar{q}$ mass.

Events containing additional fermion pairs from radiative processes are considered to be signal, providing that the primary pair passes the cut on $\sqrt{s'/s}$ and that the secondary pair has a mass below 70 GeV/$c^2$.

| Year | Nominal Energy GeV | Actual Energy GeV | Luminosity $pb^{-1}$ |
|---|---|---|---|
| 1995 | 130 | 130.2 | $\sim 3$ |
| | 136 | 136.2 | $\sim 3$ |
| | 133* | 133.2 | $\sim 6$ |
| 1996 | 161 | 161.3 | $\sim 10$ |
| | 172 | 172.1 | $\sim 10$ |
| | 167* | 166.6 | $\sim 20$ |
| 1997 | 130 | 130.2 | $\sim 2$ |
| | 136 | 136.2 | $\sim 2$ |
| | 183 | 182.7 | $\sim 50$ |
| 1998 | 189 | 188.6 | $\sim 170$ |
| 1999 | 192 | 191.6 | $\sim 30$ |
| | 196 | 195.5 | $\sim 80$ |
| | 200 | 199.5 | $\sim 80$ |
| | 202 | 201.6 | $\sim 40$ |
| 2000 | 205 | 204.9 | $\sim 60$ |
| | 207 | 206.7 | $\sim 30$ |
| | 206* | 205.5 | $\sim 90$ |

Table 13: The nominal and actual centre-of-mass energies for data collected during LEP-II operation in each year. The approximate average luminosity analysed per experiment at each energy is also shown. Values marked with a * are average energies for 1995, 1996 and 2000 used for heavy flavour results. The data taken at nominal energies of 130 and 136 in 1995 and 1997 are combined by most experiments.

The data are split into 3 sets: data taken at energies from 130–189 GeV, data taken during 1999, and data taken in 2000. Averages are performed separately for each of these data sets. Within each subset correlations between experiments and energies and channels are considered.

Tables 14 and 15 show the preliminary combined results for the 1995–1999 data corresponding to the signal definition 1 and the difference in the results if definition 2 is used. The results for the averages of the 130–189 GeV data are identical to those given in [72]. Results for the more preliminary data taken during 2000 are not given in numerical form but are shown in Figure 3 which show the LEP averaged cross sections and asymmetries (based on definition 1), respectively, as a function of the centre-of-mass energy, together with the SM predictions.

The $\chi^2$ per degree of freedom for the average of the 1999 data is 52.5/60. The correlations are rather small, with the largest components at any given pair of energies being between the hadronic cross sections.

There is good agreement between the SM expectations and the measurements of the individual experiments and the combined averages. The cross sections for hadronic final states at most of the energy points are somewhat above the SM expectations. Taking into account the correlations between the data points and also assigning a theory error of $\pm 0.2\%$ [73] to the SM predictions, the difference of the cross section from the SM expectations averaged over all energies is approximately a 2.5 standard deviation excess. It is concluded that there is no significant evidence in the results of the combinations for physics beyond the SM in the process $e^+e^- \to f\bar{f}$.

| $\sqrt{s}$ (GeV) | Quantity | Value | SM | $\Delta$ |
|---|---|---|---|---|
| 130 | $\sigma(q\overline{q})$ [pb] | 81.938±2.220 | 82.803 | -0.251 |
| | $\sigma(\mu^+\mu^-)$ [pb] | 8.592±0.682 | 8.439 | -0.331 |
| | $\sigma(\tau^+\tau^-)$ [pb] | 9.082±0.931 | 8.435 | -0.108 |
| | $A_{fb}(\mu^+\mu^-)$ | 0.692±0.060 | 0.705 | 0.012 |
| | $A_{fb}(\tau^+\tau^-)$ | 0.663±0.076 | 0.704 | 0.012 |
| 136 | $\sigma(q\overline{q})$ [pb] | 66.570±1.967 | 66.596 | -0.224 |
| | $\sigma(\mu^+\mu^-)$ [pb] | 8.231±0.678 | 7.281 | -0.280 |
| | $\sigma(\tau^+\tau^-)$ [pb] | 7.123±0.821 | 7.279 | -0.091 |
| | $A_{fb}(\mu^+\mu^-)$ | 0.704±0.060 | 0.684 | 0.013 |
| | $A_{fb}(\tau^+\tau^-)$ | 0.752±0.088 | 0.683 | 0.014 |

Table 14: Preliminary combined LEP results for $e^+e^- \to f\overline{f}$ for centre-of-mass energies below the W–pair production threshold. All the results correspond to the signal definition 1. The Standard Model predictions are from ZFITTER v6.10 [74]. The difference, $\Delta$, in the averages for the measurements for definition 2 relative to definition 1 are also indicated. The quoted uncertainties do not include the theoretical uncertainties on the corrections discussed in [70]

### 7.2 Differential cross sections

The LEP experiments have measured the differential cross section, $\frac{d\sigma}{d\cos\theta}$, for the $e^+e^- \to \mu^+\mu^-$ and $e^+e^- \to \tau^+\tau^-$ channels. This section discusses a procedure to combine these measurements and presents preliminary results.

Using a Monte Carlo simulation it is found that a $\chi^2$ fit to the measured differential cross sections, using the expected error on the differential cross sections, computed from the expected cross sections and the expected numbers of events in each experiment, provided a very good approximation to the exact likelihood method based on Poisson statistics. Further details are given in [70].

Data are binned in 10 bins of $\cos\theta$. The scattering angle, $\theta$, is the angle of the negative lepton with respect to the incoming electron direction in the lab coordinate system. The outer acceptances of the most forward and most backward bins for which the four experiments have presented their data are different. This is accounted for as a correction to a common signal definition. The signal definition used corresponds to definition 1 of Section 7.1.

Correlated small systematic errors between different experiments, channels and energies, arising from uncertainties on the overall normalisation are considered.

The data are subdivided into two energy ranges, 183 and 189 GeV and 192–202 GeV, and averages are made for each energy point within each of these subsets. The results of the averages are shown in Figures 4 and 5.

The correlations between bins in the average are less that 2% of the total error on the averages in each bin. The overall agreement between the averaged data and the predictions is good, with a $\chi^2$ of 114 for 120 degrees of freedom. At 202 GeV the cross section in the most backward bin, $-1.00 < \cos\theta < -0.8$, for both muon and tau final states is above the predictions. For the muons the excess in data corresponds to 3.3 standard deviations. For the taus the excess is 2.3 standard deviations, however, for this measurement the individual experiments are somewhat inconsistent, having a chi-squared with respect to the average of 10.5 for 2 degrees of freedom.

| $\sqrt{s}$ (GeV) | Quantity | Value | SM | $\Delta$ |
|---|---|---|---|---|
| 161 | $\sigma(q\overline{q})$ [pb] | 36.909±1.071 | 35.247 | -0.143 |
| | $\sigma(\mu^+\mu^-)$ [pb] | 4.586±0.364 | 4.613 | -0.178 |
| | $\sigma(\tau^+\tau^-)$ [pb] | 5.692±0.545 | 4.613 | -0.061 |
| | $A_{\rm fb}(\mu^+\mu^-)$ | 0.535±0.067 | 0.609 | 0.017 |
| | $A_{\rm fb}(\tau^+\tau^-)$ | 0.646±0.077 | 0.609 | 0.016 |
| 172 | $\sigma(q\overline{q})$ [pb] | 29.172±0.987 | 28.738 | -0.124 |
| | $\sigma(\mu^+\mu^-)$ [pb] | 3.556±0.317 | 3.952 | -0.157 |
| | $\sigma(\tau^+\tau^-)$ [pb] | 4.026±0.450 | 3.951 | -0.054 |
| | $A_{\rm fb}(\mu^+\mu^-)$ | 0.672±0.077 | 0.591 | 0.018 |
| | $A_{\rm fb}(\tau^+\tau^-)$ | 0.342±0.094 | 0.591 | 0.017 |
| 183 | $\sigma(q\overline{q})$ [pb] | 24.567±0.421 | 24.200 | -0.109 |
| | $\sigma(\mu^+\mu^-)$ [pb] | 3.484±0.147 | 3.446 | -0.139 |
| | $\sigma(\tau^+\tau^-)$ [pb] | 3.398±0.174 | 3.446 | -0.050 |
| | $A_{\rm fb}(\mu^+\mu^-)$ | 0.558±0.035 | 0.576 | 0.018 |
| | $A_{\rm fb}(\tau^+\tau^-)$ | 0.608±0.045 | 0.576 | 0.018 |
| 189 | $\sigma(q\overline{q})$ [pb] | 22.420±0.248 | 22.156 | -0.101 |
| | $\sigma(\mu^+\mu^-)$ [pb] | 3.109±0.077 | 3.207 | -0.131 |
| | $\sigma(\tau^+\tau^-)$ [pb] | 3.140±0.100 | 3.207 | -0.048 |
| | $A_{\rm fb}(\mu^+\mu^-)$ | 0.565±0.021 | 0.569 | 0.019 |
| | $A_{\rm fb}(\tau^+\tau^-)$ | 0.584±0.028 | 0.569 | 0.018 |
| 192 | $\sigma(q\overline{q})$ [pb] | 22.292±0.514 | 21.237 | –0.098 |
| | $\sigma(\mu^+\mu^-)$ [pb] | 2.941±0.175 | 3.097 | –0.127 |
| | $\sigma(\tau^+\tau^-)$ [pb] | 2.863±0.216 | 3.097 | –0.047 |
| | $A_{\rm FB}(\mu^+\mu^-)$ | 0.540±0.052 | 0.566 | 0.019 |
| | $A_{\rm FB}(\tau^+\tau^-)$ | 0.610±0.071 | 0.566 | 0.019 |
| 196 | $\sigma(q\overline{q})$ [pb] | 20.730±0.330 | | |